Journal of Alloys and Compounds 455 (2008) 269–273

Journal of ALLOYS AND COMPOUNDS

www.elsevier.com/locate/jallcom

Growth and spectroscopy of $ZnWO_4:Ho^{3+}$ crystal

Fugui Yang [a,b,c], Chaoyang Tu [a,b,*], Hongyan Wang [a,b,c], Yanping Wei [a,b,c], Zhenyu You [a,b], Guohua Jia [a,b], Jianfu Li [a,b], Zhaojie Zhu [a,b], Xiuai Lu [a,b,c], Yan Wang [a,b]

[a] The State Key Laboratory of Structural Chemistry, PR China
[b] Fujian Institute of Research on the Structure of Matter, Chinese Academy of Sciences, Fuzhou, Fujian 350002, PR China
[c] Graduated School of Chinese Academy of Sciences, Beijing 100039, PR China

Received 31 May 2006; received in revised form 25 December 2006; accepted 5 January 2007
Available online 11 January 2007

Abstract

The single crystal of $ZnWO_4:Ho^{3+}$ was grown by Czochralski technique. The XRD, absorption spectra, fluorescence spectrum are presented, and the Judd–Ofelt (J–O) intensity parameters Ω_2, Ω_4, Ω_6 are obtained to be 4.61×10^{-20} cm^2, 0.16×10^{-20} cm^2, 0.48×10^{-20} cm^2, respectively. Calculated radiative transition rate, branching ratios, and radiative lifetime for different transition levels of $ZnWO_4:Ho^{3+}$crystals are presented. The most intense line correlative with the transition $^5S_2 \rightarrow {}^5I_8$ at 543 nm is potentially used for green solid state laser, and the fluorescence lifetime of this energy level is 14.1 μs.

PACS: 71.20.Eh; 78.20.−e

Keywords: Spectroscopy; Czochralski method; $ZnWO_4:Ho^{3+}$

1. Introduction

Holmium ion is known as the activator to lase at 2 μm and 0.55 μm. The main interest in 2 μm corresponding to transition $^5I_7 \rightarrow {}^5I_8$ is for the use as an eye-safe source in atmosphere, medicine, wind shear, laser radar . . . [1–4]. The green emission corresponding to transition $^5S_2 \rightarrow {}^5I_8$, centered at 0.55 μm, has been observed, and can be utilized as a visible solid-state laser [5,6]. The ground state of Ho^{3+} is $^5I_8$, and the excited states are $^5I_7$, $^5I_6$, $^5I_5$, $^5I_4$, $^5F_5$, $^5F_4$, $^5G_6$, $^5G_5$, $^3H_6$ . . ..

Crystal $ZnWO_4$ has the monoclinic structure with *P*2/*c* space group. Its lattice parameters $a = 0.469263(5)$ nm, $b = 0.572129(7)$ nm, $c = 0.492805(5)$ nm, and $\beta = 90.6321(9)°$ [7]. In this work, single crystal of $ZnWO_4:Ho^{3+}$ was grown by Czochralski technique, and the spectroscopy was presented.

2. Experimental procedures

Using pure ZnO (99.9%), WO_3 (99.9%), Ho_2O_3 (99.97%), single crystal $ZnWO_4:Ho^{3+}$ was grown by the Czochralski technique. Here, the doped concentration of Ho^{3+} is 2 at%. The initial compounds were mixed in a carnelian bowl, and sintered for almost 3–5 days at 1010 °C. Then the charge was deposited in a Pt crucible bowl of Ø 55 mm × 30 mm, and placed in the DJL-400 furnace. The crystal was grown with the Pt-wire rotating at a rate of 8–12 rpm, and at a pulling rate of 1.2 mm/h. When the procedure was over, the crystal was drawn out, and cooled down to room temperature at a rate of 10–25 °C/h. Finally, the single-crystals $ZnWO_4:Ho^{3+}$ with size of Ø 20 mm × 25 mm were obtained.

The X-ray powder diffraction investigations are carried out with CAD4 diffractometer, equipped with Cu Kα radiation (λ = 1.54056 Å). The data are collected using Ni-filtered Cu-target tube at room temperature in the 2θ range from 5° to 85°. Fig. 1 shows the diffraction patterns, which is in good accordance with the standard JCPDS card (No. 73 0554) of $ZnWO_4$ [8].

The crystal was oriented by YX-2 X-ray Crystal Orientation Unit produced by Dandong Radioactive Instrument Co. Ltd., and was cut into several samples. Samples used for spectroscopic measurements are optically polished to flat.

Fig. 2 shows the room temperature absorption spectra of crystal $ZnWO_4:Ho^{3+}$ measured by Lamda900 spectrometer (Perkin-Elmer UV-VIS Spectrometer) along three crystallographic axes. The samples are flat with the heights of 1.68 mm, 1.62 mm, and 1.64 mm along *a*, *b*, *c* directions, respectively. The fluorescence spectrum recorded by FLS920 at room temperature excited by 445 nm, using a CW xenon lamp as the exciting source, is shown in Fig. 3. The

* Corresponding author at: Fujian Institute of Research on the Structure of Matter, Chinese Academy of Sciences, Fuzhou, Fujian 350002, PR China. Tel.: +86 591 8371 1368/2122; fax: +86 591 8371 4946.
E-mail address: tcy@fjirsm.ac.cn (C. Tu).

0925-8388/$ – see front matter © 2007 Elsevier B.V. All rights reserved.
doi:10.1016/j.jallcom.2007.01.011

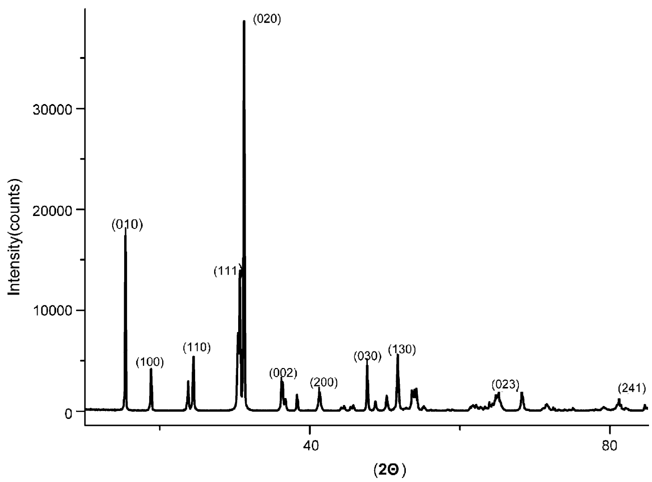

Fig. 1. X-ray powder diffraction pattern of $ZnWO_4$:Ho^{3+} crystal.

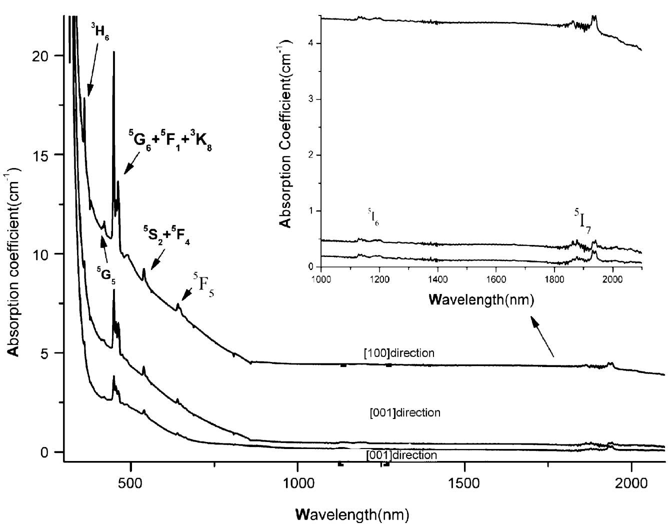

Fig. 2. Absorption spectra along *a*, *b*, *c* directions of crystal $ZnWO_4$:Ho^{3+}. The *y*-axis expresses absorption coefficient; the *x*-axis is the wavelength.

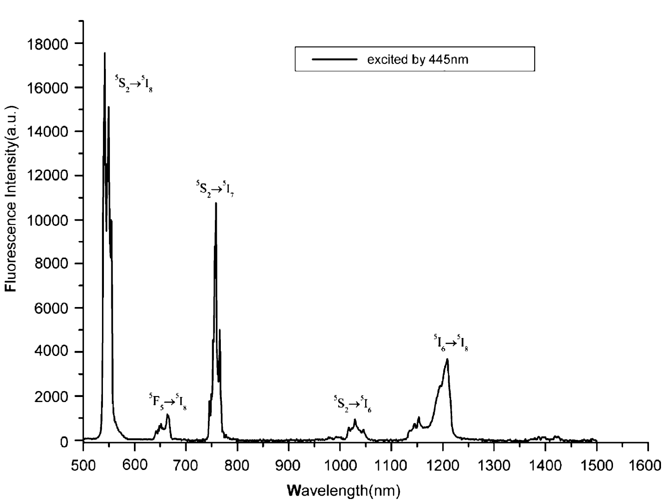

Fig. 3. Room temperature fluorescence spectrum of $ZnWO_4$:Ho^{3+} excited with 445 nm.

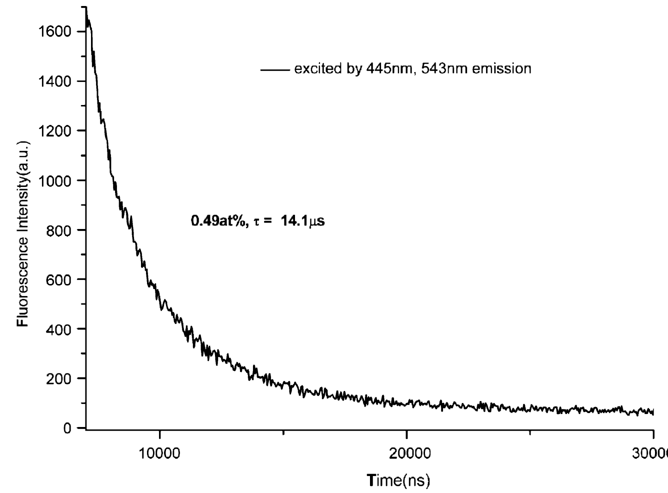

Fig. 4. Room temperature fluorescence decay curve excited by 445 nm, the *y*-axis is the fluorescence intensity, and the *x*-axis shows the time (ns).

height of the used sample is 1.62 mm. The fluorescence decay lifetime curve correlative with $^5S_2$ at 543 nm is shown in Fig. 4, and τ_f is measured to be 14.1 μs.

3. Results and discussion

The concentration of Ho^{3+} in $ZnWO_4$ was measured to be 0.26 wt% (0.49 at%) by inductively coupled plasma atomic emission spectrometry method (ICP-AES instrument). So, the calculation of segregation coefficients of the dopant in crystals *K* was performed by the following formula:

$$K = \frac{(\text{molesHo}/(\text{molesHo} + \text{molesZnWO}_4))_{\text{crystal}}}{(\text{molesHo}/(\text{molesHo} + \text{molesZnWO}_4))_{\text{melt}}} \quad (1)$$

Here, molesHo, and molesZnWO_4 are the mole fraction of dopant and trivalent host ion, respectively, in the crystal (numerator), and in the melt (denominator). The segregation coefficient of Ho^{3+} in $ZnWO_4$ was obtained to be 0.24.

The monoclinic structure of $ZnWO_4$:Ho^{3+} crystal exhibits typical anisotropic characteristic. Thus, it is important to investigate the spectroscopy along three crystallographic axes. Fig. 2 shows the absorption spectra along [1 0 0] [0 1 0] [0 0 1] at room temperature. Along [1 0 0] direction, the base line moves away. The phenomenon could be explained by the natural [1 0 0] slip face in the structure of $ZnWO_4$. The absorption peaks are almost in the region of 300–800 nm. Five apparent transition peaks centered at 361 nm, 421 nm, 445 nm, 538 nm, and 641 nm are correlative with the transitions of $^5I_8 \rightarrow {}^3H_6$, $^5I_8 \rightarrow {}^5G_5$, $^5I_8 \rightarrow {}^5G_6 + {}^5F_1 + {}^3K_8$, $^5I_8 \rightarrow {}^5F_4 + {}^5S_2$, and $^5I_8 \rightarrow {}^5F_5$, respectively. The transition of $^5I_8 \rightarrow {}^5G_6 + {}^5F_1 + {}^3K_8$ centered at 445 nm could be bumped to emit 0.55 μm green laser. Zooming in the region of the infrared band, two peaks centered at 1128 nm and 1929 nm are found, which correlative with the transition of $^5I_8 \rightarrow {}^5I_6$ and $^5I_8 \rightarrow {}^5I_7$. The transition of $^5I_8 \rightarrow {}^5I_7$ could be bumped to emit 2.0 μm eye-safe laser. The absorption cross-section is calculated by the following equations:

$$\sigma_a = \frac{a}{N_c} \quad (2)$$

Table 1
Integrated absorbance Γ along three crystallographic axes of $ZnWO_4:Ho^{3+}$

Excited state (ground state $^5I_8$)	Wavelength (nm)	Γ (nm/cm)			$\overline{\Gamma(\lambda)}$ (nm/cm)
		a	*b*	*c*	
$^3H_6$	361	5.52	0.22	0.63	2.12
$^5G_5$	421	1.64	0.53	0.22	0.79
$^3K_8+^5F_1+^5G_6$	445	64.04	12.02	26.67	34.24
$^5S_2+^5F_4$	538	2.56	1.13	2.19	1.96
$^5F_5$	641	2.46	1.03	1.39	1.63
$^5I_6$	1128	3.27	3.20	3.38	3.28
$^5I_7$	1929	30.99	12.13	16.49	19.87

$$a = \frac{A}{L\ \log\ e} \tag{3}$$

Here, σ_a is the absorption cross-section; a is the absorption coefficient, A is the absorbance, L is the thickness of the polished crystal, and N_c is the doped ion concentration (here is 0.49 at%) in atoms. Based on the absorption spectra, the absorption cross-section versus wavelength was obtained. At 445 nm, the absorption cross-sections σ_a along a, b, c axes are $15.5\times10^{-20}\ cm^2$, $3.7\times10^{-20}\ cm^2$, and $7.3\times10^{-20}\ cm^2$, respectively. The average is $8.8\times10^{-20}\ cm^2$. The absorption cross-sections centered at 1929 nm, correlative with transition $^5I_8\rightarrow{}^5I_7$ and are $6.0\times10^{-20}\ cm^2$, $0.34\times10^{-20}\ cm^2$, and $0.55\times10^{-20}\ cm^2$, respectively.

The experimental data obtained from the absorption spectra are used to calculate the oscillator strengths. The experimental oscillator strength f_{exp} can be calculated by using the following formula:

$$f_{exp} = \frac{mc^2\Gamma}{\pi e^2 N_0 L \lambda^2} \tag{4}$$

$$\Gamma = \frac{\int D(\lambda)\,d\lambda}{L\ \log\ e} = \frac{2.303\int D(\lambda)\,d\lambda}{L} \tag{5}$$

where N_0 is the concentration of Ho^{3+}; L is the thickness; n is the refractive index to be 2.25; Γ is the integrated absorbance for each absorption band; $D(\lambda)$ is the absorbance. The integrated absorbance Γ associated with the seven transitions was calculated as shown in Table 1.

Based on the Judd–Ofelt theory, the measured line strengths are then used to obtain the J–O intensity parameters Ω_2, Ω_4, and Ω_6 by fitting the set of equations from the corresponding transitions between J and J′ manifolds in the following equation:

$$S_{meas}(J\rightarrow J') = \frac{(2J+1)}{N_0}\frac{3hc}{8\pi^3\lambda e^2}\frac{9n}{(n^2+2)^2}\bar{\Gamma} \tag{6}$$

$$S_{calc}(J\rightarrow J') = \sum_{t=2,4,6}\Omega_t\left|\left\langle(S,L)J\left\|U^{(t)}\right\|(S',L')J'\right\rangle\right|^2 \tag{7}$$

$$S_{calc} = U\Omega \tag{8}$$

where $U^{(t)}$ ($t=2$, 4, 6) are the matrix elements of unit tensor that have been calculated by Carnall et al. [9]. The root mean square (rms) deviation between experimental, and calculated line strengths is determined by

$$\text{rms}\Delta S = \sqrt{\sum_{t=1}^{N}(S_{meas}-S_{calc})^2/(N-3)} \tag{9}$$

where

$$\text{rms}S = \sqrt{\sum_{i=1}^{N}S_{meas}^2/N} \tag{10}$$

So, the rms error is $0.25\times10^{-20}\ cm^2$.

After a least-square fitting of S_{meas} to S_{calc}, the three J–O intensity parameters were obtained: $\Omega_2=4.61\times10^{-20}\ cm^2$, $\Omega_4=0.16\times10^{-20}\ cm^2$, and $\Omega_6=0.48\times10^{-20}\ cm^2$. The three J–O intensity parameters compared with other Ho^{3+}-doped crystals are shown in Table 2, [10–13]. The values of J–O parameters depend on the crystal structure. From the comparison, we can find that the values of Ω_4 and Ω_6 are smaller, which indicates the component of covalent bond is also smaller.

From the 4f–4f intensity model, the calculated oscillator strength of a transition between two multiplets is defined as [14]:

$$f_{cal} = \frac{8\pi^2 mc}{3h\lambda(2J+1)}\frac{(n^2+2)^2}{9n} \times\sum_{t=2,4,6}\Omega_t\left\langle 4f^n(\alpha'S'L')J'||U^{(t)}||4f^n(\alpha SL)J\right\rangle^2 \tag{11}$$

Table 2
The J–O intensity parameters of Ho^{3+}-doped crystals

Crystal	Ω_2 ($10^{-20}\ cm^2$)	Ω_4 ($10^{-20}\ cm^2$)	Ω_6 ($10^{-20}\ cm^2$)	Reference
$LaAlO_3$	5.362	1.862	1.065	[10]
$YAlO_3$	1.82	2.38	1.53	[11]
YAG	0.04	2.67	1.89	[12]
LuAG	0.172	2.08	1.92	[13]
$ZnWO_4$	4.61	0.16	0.48	This work

Table 3
Electrical dipole line strengths and oscillator strengths of $ZnWO_4:Ho^{3+}$ crystal

Excited states	λ (nm)	Line strength (10^{-20} cm^2)		Oscillator strength (10^{-6})	
		S_{exp}	S_{cal}	f_{exp}	f_{cal}
$^5I_7$	1929	1.005	0.862	0.819	0.702
$^5I_6$	1128	0.284	0.375	0.395	0.522
$^5F_5$	641	0.248	0.338	0.608	0.829
$^5S_2+{}^5F_4$	538	0.355	0.483	1.038	1.411
$^3K_8+{}^5F_1+{}^5G_6$	445	7.437	7.377	26.035	25.826
$^5G_5$	421	0.183	0.085	0.683	0.317
$^3H_6$	361	0.573	1.012	2.494	4.408

Table 4
Calculated radiative transition rate, branching ratios, and radiative lifetime for different transition levels of $ZnWO_4:Ho^{3+}$ crystal

Start levels	Terminal levels	Wavelength (nm)	A (s^{-1})	β	τ_r (μs)
$^5S_2$	$^5F_5$	2979	0.23	1.08×10^{-4}	463
	$^5I_6$	1028	127.44	0.06	
	$^5I_7$	757	812.47	0.37	
	$^5I_8$	543	1220	0.56	
$^5F_5$	$^5I_6$	1569	64.61	0.05	780
	$^5I_7$	1014	267.78	0.21	
	$^5I_8$	664	948.25	0.74	
$^5I_7$	$^5I_8$	1920	73.20	1	13660

$$\text{rms} f = \sqrt{\sum_{i=1}^{N} \left| f_{cal} - f_{exp} \right|^2 / N} \tag{12}$$

Then, the experimental oscillator strength f_{exp}, and calculated oscillator strength f_{cal} were obtained. The error rms$f$ is obtained to be 0.7×10^{-6}. Table 3 lists the experimental, and calculated line strength S_{meas}, S_{calc}, the oscillator f_{exp}, and f_{calc}.

The fluorescence spectrum of the crystal excited by 445 nm recorded at room temperature is shown in Fig. 3. In the spectra, five intense emission peaks at 543 nm, 664 nm, 757 nm, 1028 nm, and 1208 nm are corresponding to the transitions $^5S_2\rightarrow{}^5I_8$, $^5F_5\rightarrow{}^5I_8$, $^5S_2\rightarrow{}^5I_7$, $^5S_2\rightarrow{}^5I_6$, $^5I_6\rightarrow{}^5I_8$ of Ho^{3+} ions, respectively. The most intense line at 543 nm with FWHM of 13 nm is potentially used for green laser.

Using the obtained emission line strengths, the radiative decay rates $A(J\rightarrow J')$ can be determined by the following equations [15]:

$$A(J\rightarrow J') = \frac{64\pi^4 e^2}{3h(2J+1)\bar{\lambda}^3}\frac{n(n^2+2)^2}{9} \times \sum_{t=2,4,6} \Omega_t \left| \langle (S,L)J \left\| U^{(t)} \right\| (S',L')J' \rangle \right|^2 \tag{13}$$

$$A_T(J) = \sum_{J'} A(J\rightarrow J') \tag{14}$$

Then the radiative lifetimes $\tau_r = 1/A_T(J)$, the mathematical formula for the fluorescent branching ratio is found by:

$$\beta(J') = \frac{A(J\rightarrow J')}{A_T(J)} \tag{15}$$

The calculated radiative transition rate, the branching ratios, and the radiative lifetime for different transition levels are presented in Table 4. The stimulated emission cross-section σ_p related to the radiative transition probability can be defined as:

$$\sigma_p = \frac{A(J\rightarrow J')\lambda_p^2}{4\pi^2 n^2 c\Delta\nu} \tag{16}$$

Here, the full frequency width at half maximum is $\Delta\nu$; λ_p is the vacuum wavelength of the emission peak. Therefore, the emission cross-section σ_p centered at 543 nm is calculated to be 0.14×10^{-20} cm^2.

Fig. 4 shows the fluorescence decay curve excited by 445 nm at room temperature in correspondence with the emission line $^5S_2\rightarrow{}^5I_8$ at 543 nm. The fluorescence lifetime τ_f was measured to be 14.1 μs, and the radiative lifetime τ_r of the $^5S_2$ level was calculated to be 463 μs. The decay lifetime curve is almost single exponential, and apparently shorter than the radiative transitions calculated from the J–O theory. The phenomenon is probably from intense cross-relaxations down and up conversions $\sigma_p\tau_f$ at 543 nm correlative with transition $^5S_2\rightarrow{}^5I_8$ is 1.97×10^{-26} cm^2 s.

4. Conclusion

Single-crystal $ZnWO_4:Ho^{3+}$ was grown by Czochralski technique. The absorption spectra along three crystallographic axes were measured at room temperature. Along three axes, anisotropic optical absorption characteristics are presented, and in the [1 0 0] direction, the baseline moves away due to the existence of slip faces in the structure of $ZnWO_4$. Room temperature fluorescence spectrum was measured and discussed. The most intense line at 543 nm corresponding to transition $^5S_2 \rightarrow {}^5I_8$ is found, whose emission cross-section is 0.14×10^{-20} cm^2, and the fluorescence lifetime τ_f of this energy level is measured to be 14.1 μs.

Acknowledgements

This project was supported by the Innovative Project of Chinese Academy of Sciences (KJCX2-SW-h05) and the Natural Science Foundation of the Fujian Province of China.

References

[1] M.E. Storm, Laser Focus World 27 4 (1991) 117.
[2] B. Struve, G. Huber, J. Phys. IV 1 (1991) 3.
[3] K. Azawu, Rev. Laser Eng. 26 (2000) 291.
[4] T. Becker, G. Hiber, H.J.V.D. Heide, P. Mitzscherlich, B. Struve, E.W. Duczynski, Opt. Commun. 801 (1990) 47.
[5] I.G. Podkolzina, A.M. Tkaczuk, V.A. Fedorov, P.P. Feofilov, Opt. Spektrosc. 40 (1976) 196.
[6] A.A. Kaminskii, V.M. Garmosh, G.A. Ermakov, V.A. Akkerman, A.A. Filmonov, K. Kurbarov, Izv. Akad. Nauk SSSR Ser. Neorg. Mater. 22 (1986) 1576.
[7] P.F. Schofield, K.S. Knight, G. Cressey, J. Mater. Sci. 31 (1996) 2873.
[8] O.S. Filipenko, E.A. Pobedimskaya, N.V. Belov, Kristallografiya 13 (1968) 163.
[9] W.T. Carnall, P.R. Fields, K. Rajnak, J. Chem. Phys. 49 (1968) 4424.
[10] P.J. Derén, J-C. Krupa, J. Alloy. Compd. 380 (2004) 362.
[11] E. Rukmini, C.K. Jayasanker, Opt. Mater. 4 (1995) 529.
[12] M. Malinowski, Z. Frukacz, M. Szuflinska, A. Wnuk, M. Kaczkan, J. Alloy. Compd. 300 (2000) 389.
[13] D.N. Patel, B.R. Brody, S.K. Nash-Stevenson, Opt. Mater. 10 (1998) 225.
[14] W.T. Carnall, H. Crosswhite, H.M. Crosswhit, Argone National Laboratory Special Report, 1977.
[15] W.F. Krupke, IEEE J. Quantum Electron. QE-10 (1974) 450.